Characterization of wide-gap semiconductors by photothermal deflection spectroscopy

Masatomo Sumiya*

National Institute for Materials Science, 1-1 Namiki Tsukuba, Ibaraki 305-0044, Japan

*E-mail: SUMIYA.Masatomo@nims.go.jp

III-V nitride semiconductors have been characterized by photothermal deflection spectroscopy (PDS) in my research group. After understanding the challenges of applying PDS to materials emitting light, we describe the advantages and features of PDS for evaluating the defect level in the band gap of III-V nitride semiconductors. The reciprocal of the slope of the PDS spectrum near the bandgap energy (Urbach-like energy) increased with increasing indium composition in InGaN film. According to the larger Urbach-like energy, the radial distribution determined by x-ray absorption fine structure was likely to be decreased. This was possibly attributed to the N vacancies or the random arrangement of In atom in InGaN film. Also, it was proposed that the Urbach-like energy should be considered when the in-gap emission caused by defects was discussed. Photothermal deflection spectroscopy can provide the information of non-radiative recombination involving defect levels for understanding the knowledge about the defects in III-V nitride semiconductors.

1. Introduction

Defects due to dislocations, impurities, and vacancies in semiconductors affect physical properties and device characteristics. Therefore, intensive efforts have being made to fabricate materials with few defects that exhibit good physical properties such as strong photoluminescence (PL) and high mobility. Group III-V nitride semiconductors for blue LEDs emit light well even with many dislocations (defects). [1] However, it is very important to study defect in the band gap of III-V nitride semiconductors for improving the performance in UV-[2,3] and long-wavelength[4] LEDs, HEMTs[5], and vertical power electronic devices[6].

III-V nitride semiconductor materials are conventionally characterized by the full width at half maximum (FWHM) of the rocking curve of x-ray diffraction. Better samples are often subjected to the detailed defect evaluations. There are many methods for evaluating defects in semiconductor materials. Structural defects such as dislocations can be analyzed by Burgers vector obtained by transmission electron microscopy.[7] The elements and its amount of impurity can be evaluated from the isotope ratio and intensity in secondary ion mass spectroscopy.[8] Although nitrogen vacancies (V_N) are difficult to detect, Ga vacancy-type (V_{Ga}) defects are detected by positron annihilation spectroscopy.[9] These various defects form defect levels in the band gap of the semiconductor, and their influences are reflected in physical properties. For example, depending on the type and density of defects, the PL intensity and lifetime at the band edge change.[10] A deep defect level works as a path for leakage current, degrading device characteristics of photo diode or a transistor. Therefore, the measurements of the defect level and its density in the band gap can be a means of judging the quality of semiconductor materials and devices.

Deep-level transient spectroscopy (DLTS) is a well-known method for detecting deep defect levels up to ~0.6 eV in the band gap of Si. In III-V nitride semiconductors, DLTS can be applied to measure the defect levels formed in ~1.0 eV from the bottom of the conduction band (E_c).[11] In order to detect the defect levels in the bandgap of group III-V nitrides more deeply, my research group applied photothermal deflection spectroscopy (PDS)[12], which was used for defect characterization of hydrogenated amorphous silicon (a-Si:H). This

method does not require the junctions such as p-n and Schottky barrier diode using metal electrodes for detecting the defect levels. It has the feature that the absorption coefficient in the band gap of semiconductors can be estimated. Defect characterization by PDS for III-V nitride semiconductors is not very familiar. PDS method is not well-known what kind of defect it can detect, and what kind of ability it has.

In this paper, the potential of PDS is described for evaluating defect levels in the band gap of III-V nitride semiconductors. While comparing the other methods to characterize the defects in III-V nitride semiconductors, we will discuss the challenges we experienced through using PDS technique. The correlation between the PDS spectra of InGaN films and the radial distribution of In-In atoms obtained from x-ray absorption fine structure (XAFS) will be discussed with respect to Urbach energy. Since PDS (nonradiative process) is contrary to photoluminescence (radiative process), the correlation between the emission related to the defect levels determined by PDS will be discussed. After describing the features and problems of PDS, we introduce interpretations of defect levels in the bandgap of III-V nitride semiconductors from both radiative (PL) and non-radiative (PDS) recombination processes.

2. Experimental methods

InGaN films with a thickness of 0.2–0.3 μm were grown on c-sapphire by horizontal metal–organic chemical vapor deposition (MOCVD) under atmospheric pressure. After growing a GaN layer (~2 μm thick) for 1 h at 1000 ◦C on various substrates of c-sapphire, Si (111) or bulk GaN, the atmosphere inside the MOCVD reactor was changed from H_2 to N_2 for the InGaN film growth. An $In_{0.03}Ga_{0.97}N$ film (0.1 μm thick) as an interlayer was grown at 830 ◦C for 30 min on the GaN film. Thick $In_xGa_{1-x}N$ films were then grown at temperatures from 760 to 830 ◦C for 1 h under trimethylgallium, trimethylindium, and NH_3 gas at a flow rate of 7 l/min using a constant In/(Ga+In) molar ratio of 0.95. The InN mole fraction was changed only by the growth temperature and was estimated from the X-ray diffraction (XRD) of the films taking the strain effect into account.

In the PDS system used here, the sample surface was irradiated with monochromatic light

from an ozone-free solar simulator Xe lamp (350–800 nm) as a pumping source at a normal angle with a chopping frequency of 11 Hz. The pumping light was focused through a cylindrical lens with dimensions of 1 × 10 mm^2. A semiconductor laser (660 nm) as a probe was run on the sample surface in parallel, and the position of the probing laser was deflected according to the thermal energy converted from nonradiative recombination of electrons excited by the pumping light. The details are described in Ref. 13.

X-ray absorption fine structure measurements for InGaN samples were carried out on the beam-lines of BL01B1 at SPring-8. The X-ray generated from the storage ring was monochromated by two Si (311) crystals and irradiated on the sample. Fluorescence X-rays of the In K-edge were obtained from the sample and detected using a 19-element Ge solid-state detector.

3. Results and discussion

3.1 Defect evaluation by DLTS and SSPC

Table 1 shows the characteristics of the methods used for evaluating the defect levels of III-V nitride semiconductors. Schottky or pn junctions are always required for the methods of DLTS or steady-state photo-capacitance spectroscopy[14] (SSPC). These techniques utilize the fact that the capacitance of the depletion layer changes transiently when the voltage applied to the junction is changed stepwise. When the n-type semiconductor contains the defect levels that act as electron traps, a voltage in the forward direction (reducing the depletion layer) makes the levels in the band gap occupied with electrons. When a reverse bias is then applied stepwise (widening the depletion layer), electrons are emitted into the conduction band. The electrons are ejected outside the depletion layer by the electric field applied to the depletion layer. As a result, the space charge density in the depletion layer changes transiently. The change in capacitance is measured at each temperature to obtain the defect energy level as the activation energy in DLTS. Although it depends on the detection sensitivity of the capacitance measuring instrument, in the case of Si, a sample with a shallow donor density of 10^{15} cm^{-3} can be detected up to a defect level of 10^{10} cm^{-3}. The defect level energy in GaN is usually evaluated at about 0.2 to 1.0 eV from the E_c by measuring at temperatures from 77 K to 400 K. Although the detection area is limited to the depletion layer, it has the advantage of being able to evaluate defect density quantitatively.

In the measurement procedure of SSPC, a forward bias is applied so that the trap level in the depletion layer is occupied by electrons, same as DLTS. After applying a reverse bias, monochromatic light is irradiated to eject the trapped electrons, and the variation of capacitance caused by the light irradiation is measured at a constant temperature.[15] It is possible to detect between defect levels having an energy difference corresponding to the energy of the irradiated monochromatic light. GaN can be measured by DLTS at temperatures as high as 600°C, so defect levels as deep as 1.5 eV can be detected.[16] On the other hand, in SSPC, the monochromatic light is irradiated to the sample, so the defect level in the band gap of GaN up to the valence band can be obtained at room temperature. It should be noted that unlike DLTS, it does not directly indicate the energy level from the bottom of E_c, but rather the energy difference between levels like PDS as mentioned later. In addition, it is necessary to arrange a measurement system such as depositing a transparent electrode for light irradiation or irradiating from a polished back surface. The detection limit of SSPC seems to be about 10^{14} to 10^{15} cm^{-3} from the measurement of highly insulative bulk GaN samples.[17]

Both DLTS and SSPC depend on the characteristics of Schottky and pn junctions, and cannot measure electrically inactive materials. The hole density in GaN is low due to the relatively high activation energy of the Mg acceptor level in GaN. When a depletion layer is formed, the acceptor density becomes a high value of 10^{18} cm^{-3} or more. For this reason, it is difficult to form a good Schottky junction on p-GaN, and the leakage current becomes very large especially under reverse bias. The high background acceptor density significantly reduces the detection sensitivity for deep levels. For these reasons, DLTS measurements on p-GaN are difficult. Furthermore, since AlGaN and samples with wider band gap have high insulative properties, it is difficult to measure the defect electrically.

Table 1 List of defect evaluation method for III-V nitride semiconductors.

Method	DLTS	DLOS	PAS	**PDS**
Electrodes (junction)	Must (SBD, pn)	Must (SBD, pn)	None ○	None ○

Absolute estimation of defect density	Good ◎ (~10^{11} cm^{-3})	Good ◎ (>10^{14} cm^{-3})	Non ×	Possible △
Detecting depth	Depletion layer	Depletion layer	Corresponding to abs. coeff.	Corresponding to abs. coeff.
Deep level from CBM	~1.0 eV △	0.7~4.0 eV ○	Around bandgap energy	1.0-4.9 eV ○
Material properties (p-GaN)	Require good electrical (△)	Require good electrical (△)	Not required ◎	Not required ◎

3.2 Features of PDS

Figure 1 shows the schematic illustration arranged from Ref. 18 for the defect levels formed by V_{Ga}, V_N, interstitial elements, and external factors (impurities) in the bandgap of GaN. The right side shows the spectrum of GaN obtained by PDS. With the bottom of the conduction band set to zero, the incident photon energy corresponding to the band gap energy was adjusted to the value of bandgap of GaN. (As will be described later, we believe that the PDS spectra of group III-V nitrides are observed in the valence band side, similar to SSPC.) The defect levels below the conduction band can be detected by DLTS. Defect levels above the valence band are detected by minority carrier transient spectroscopy[19] (MCTS), which measures capacitive transient response similar to DLTS by generating minority carriers with optical pulses above the bandgap.

DLTS and SSPC can cover the defect levels in a wide range from the upper valence band to the lower conduction band. However, the information around 1.5 to 2.8 eV from E_c is very few. PDS may have the potential to access to detect defect levels in the mid-gap with high sensitivity, as shown in the typical n-GaN PDS spectrum. In addition, since the signal can be detected even if semiconductor metarial is electrically insulative, it has the potential to evaluate both p-GaN and AlGaN. Photoacoustic spectroscopy[20] (PAS), in which heat generated by non-radiative recombination is detected by a microphone rather than deflection of a probe laser as in PDS, has also been used for III-V nitrides. Although it is possible to detect signals at the band edge, it is currently difficult to detect signals in the band gap.

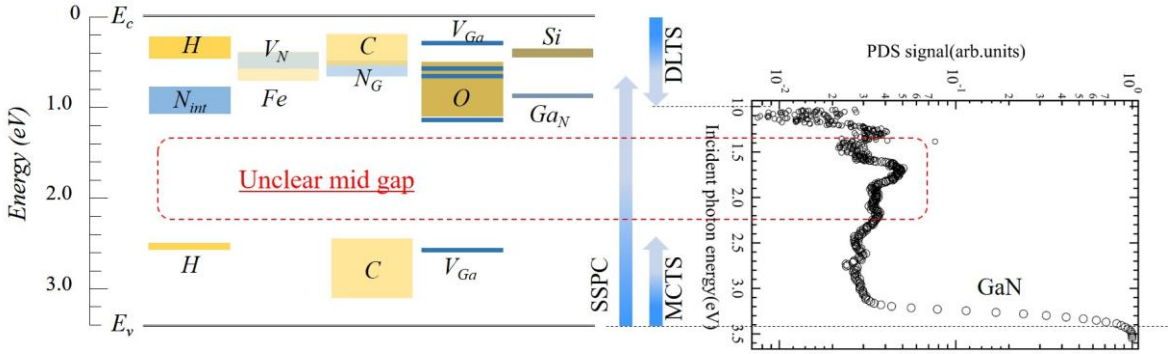

Fig. 1 Illustration of defect levels caused by intrinsic and impurities in GaN modified from Ref. 15. PDS spectrum of GaN is placed with the incident photon energy from the bottom of conduction band in the right hand.

3.3 Issues of PDS for III-V nitride semiconductors

PDS is a measurement method that utilizes the subtle deflection of a laser passing parallel to the sample surface due to the heat generated when electrons excited by monochoromatic light recombine at non-radiative centers. Since the refractive index changes due to heat generation, the sample is placed in a liquid whose refractive index changes greatly with respect to heat. Since CCl_4, commonly used in PDS measurements of a-Si:H, was found to etch the GaN surface, PDS measurements for III-V nitirdes were carried out in Fluorinert instead of CCl_4. By switching the light source between Xe lamp and halogen lamp, it is possible to measure from 1.0 eV to 4.9 eV. AlN can be evaluated by PDS if a light source with sufficient intensity at the wavelength of 200-250 nm is available.

The PDS measurement for a-Si:H was used as a technique to characterize small absorption coefficients in the band gap.[21] The PDS spectrum is obtained by integrating the density of states at the band edges and the defect states in the band gap. The slope of the sharp intensity change near the band edge is attributed to broadening of the Urbach edge due to compositional disorder.[22] This compositional disorder is defined as the reciprocal of the gradient and is an index of amorphous structural disorder as the Urbach energy. The defect levels in the band gap are due to dangling bonds in a-Si:H. The defect density can be estimated from the correlation with the intensity obtained by the method of electron spin

resonance (ESR).[23,24] Based on these concepts, PDS was applied for evaluating the defects of III-V nitrides. Since PDS is originally a method for obtaining relative absorption coefficients, it cannot be used for materials in which some of the excited electrons recombine radiatively.[25] However, the light emitting efficiency of GaN at room temperature is only a few percent, meaning that non-radiative recombination is dominated. This is why our group has used it to evaluate the defect levels of III-V nitrides. We have to pay attention to the defect evaluation of III-V nitride semiconductors by using the PDS techniques after understanding that there are various issues described below.

First, the problem is which side of the valence band or the conduction band is reflected in the signal detected by PDS. In the case of a-Si:H, the PDS spectrum was considered to reflect the conduction band side.[19-22] The PDS spectra (especially the tail state near the band gap energy) of InGaN films with different In compositions were similar to the valence band spectra observed by the hard x-ray photoemission spectroscopy (HAX-PES)[13]. From this result, we believed that the PDS signal near the band edge was derived from the electronic state close to the valence band side, although there was no method for measuring the conduction band in detail. Since the non-radiative recombination process at the top of the valence band in light-emitting materials is not well understood, the reciprocal of the slope of the top of the valence band of the PDS spectra obtained from III-V nitrides is defined as the Urbach-like energy rather than the Urbach energy.

In order to obtain the absorption coefficient in the band gap of a-Si:H, the PDS intensity at the band gap energy was matched with the absorption coefficient determined by optical absorption. This was based on the condition that a-Si:H did not emit at the band edge. It is doubtful whether the absorption coefficient in the band gap can be obtained for III-V nitrides using the same process as a-Si:H. Therefore, the PDS signal at the edge of the band has been normalized for comparison among III-V nitride samples. From our experiences, GaN sample with high defect density was likely to have large Urbach-high PDS signal in the band gap.[17]

Next issue is the sample thickness. For the PDS measurement, the thickness of a-Si:H was typically 0.1 to 1 μm. Considering the absorption coefficient, the monochromatic light

penetrates the entire film regardless of the wavelength. The thickness of GaN sample is several μm for thin film and is 400 μm or more for bulk GaN. Therefore, the penetration depth of the excited monochromatic light depends on the wavelength. As a result, the PDS signal intensity also depends on the depth. Defects existing from the substrate to the sample surface, such as threading dislocations, may enhance the PDS signal intensity. This problem will be remarkable if the defect distribution may be larger in the depth of thickness. The detection region of DLTS and SSPC is the width of the depletion layer, and the probing region by the positron annihilation method is also limited to a depth of 1 μm. Although each method can obtain a quantitative defect density, it has an own problem in understanding the defects in the entire sample.

As mentioned at the beginning of this section, in order to estimate the defect density of the a-Si:H from the absorption coefficient in the band gap of PDS spectrum, the calibration curve was obtained through measuring the dangling bond density by ESR. Since almost one defect level was detected in the band gap of a-Si:H, the correlation between the absorption coefficient and defect density was not so complicated. Since III-V nitrides have wide band gap, the various peaks are observed in the PDS spectrum as shown in Fig. 1. There is a problem that not only each level has not been identified definitively, but also the non-radiative recombination caused by the energy difference between the levels is not clearly known. It is very difficult to identify the origin of defect level and to estimate the absolute value of defect density. When the same sample of bulk GaN was evaluated by both PDS and SSPC, the PDS signal intensity qualitatively reflected the defect density.[25)]

Finally, we describe the phenomena peculiar to the PDS measurement of III-V nitride film samples. GaN film is grown on SiC and Si substrates in addition to sapphire substrates. In addition, heterostructures such as AlGaN/GaN and AlGaN/InGaN are formed for the fabrication of devices. When GaN thin films and heterostructures on substrates are evaluated by PDS, the signal from the layer with the smallest bandgap or the layer with the highest density of defects is preferentially detected. In a GaN thin film on a Si substrate, the valence band spectrum of Si is detected by PDS for a longer wavelength. In addition, signals from GaN are preferentially detected even when evaluating wide bandgap barrier layer of

AlGaN/GaN or AlInGaN/GaN heterostructures. For InGaN/GaN structures, the InGaN layer can be evaluated, but if the defect density in the band gap of the underlying GaN is high, it is necessary to be careful of the signal origin.

Although there are some problems for the evaluation of III-V nitrides by PDS as described, ion-implanted GaN samples are considered to be the most suitable for PDS measurement. This is because the depth of ion implantation is limited and many defects are introduced so that it emit no light and is also electrically inactive. The crystalline improvement of GaN region damaged by Mg ion-implantation by thermal annealing is very important for generating p-type conduction in the application of III-V nitrides to electronic devices. The Urbach-like energy obtained by PDS clearly decreased, indicating structural improvement,[26] though XRD measurement was useless due to the influence of the underlying GaN. For this reason, PDS is particularly useful for defect level evaluation of ion-implanted III-V nitride semiconductors.

In addition to III-V nitides, PDS was also applied to wide bandgap semiconductors such as Ga_2O_3 and NiO[27], which is used in the hole transport layer of perovskite solar cells. Using the chemical stability of Fluorinert, we were able to obtain a correlation between the increase in mobility of organic transistor and the improvement in Urbach energy.[28, 29]

3.4 XAFS for InGaN films

When GaN bulks with quit low values of FWHM in XRD rocking curve were measured by PDS, the Urbach-like energy for some of them was ~80 meV[25], which was worse than that of a-Si:H. It is necessary to consider what the Urbach-like energy of III-V nitrides represents. Therefore, we performed PDS and XAFS measurements of InGaN thin films with different In compositions, and compared the Urbach-like energy and radial distribution.

Figure 2(a) shows the Fourier transform results ($|\chi(R)|$) of $k3(\chi)$ for InGaN films grown on bulk GaN substrates, sapphire substrates, and Si(111) substrates. When compared to the reference InN results, the peak at the second nearest neighbor appears at a shorter radius reflecting the smaller lattice constant of InGaN. The InGaN film on the GaN bulk substrate

showed a value of FWHM of $(10\bar{1}4)$ reciprocal lattice less than 100 arcsec. On the other hand, it was 360 arcsec and 540 arcsec on the sapphire and on the Si substrate, respectively. One of the reasons of lower intensity of $|\chi(R)|$ was considered to be due to the increased fluctuations in bond angles between atoms caused by crystalline quality.

Figure 2(b) shows the radial distributions of InGaN films with different In compositions on a sapphire substrate. The intensity of the second-nearest neighbor distribution decreases significantly when the In content exceeds 10%. The values of Urbach-like energy of $In_xGa_{1-x}N$ films obtained from the PDS spectra gradually increased with increasing In content. It was 112 meV for the $In_{0.12}Ga_{0.88}N$ film. We believed that there were two possibilities for the lower radial distribution and the larger Urbach-like energy. One is the increase in V_N accompanying lower growth temperatures. Another is the fluctuation of the In atomic arrangement. The top of the valence band of III-V nitrides is composed mainly of N 2p orbitals and is hybridized with III-group elements.[30] It is possible that PDS spectra near the valence band depends on the formation of V_N and the arrangement of In atoms, which will be discussed in the next section.

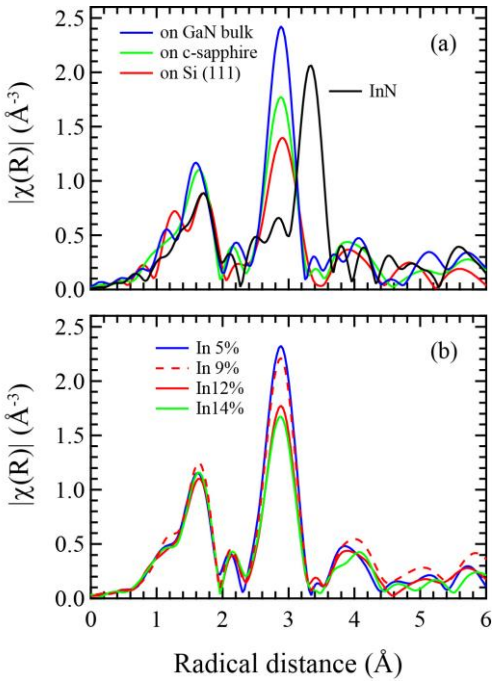

Fig. 2 Radical distribution determined by XAFS detecting In K-edgefor (a) InGaN films grown on various substrate, and (b) InGaN films with different InN mole fraction grown on sapphire substrates.

3.5 PDS and PL for InGaN films

Figure 3 shows the PDS (red) and PL spectra (blue) of InGaN thin films with different In compositions, and the Tauc plot (green) converted from the UV-VIS spectrophotometer. The GaN film sample shows a PL emission peak almost at the absorption edge (Fig. 3(a)). For $In_{0.05}Ga_{0.95}N$ film, the slope of the PDS spectrum changes at around 3.1 eV, and a tail state is observed on the low-energy side (Fig. 3(b)). For $In_{0.08}Ga_{0.92}N$ film, the strength in the tail state increased. The PL peak shifts to the energy where the slope of the PDS spectrum changes, and the energy difference between the PL peak and the absorption edge increases (Fig. 3(c)).

The decomposition efficiency of NH_3 to generate N radial decreases with low temperature growth. Low-temperature growth of InGaN films made the In composition and V_N defects increased. The valence band top must be affected by V_N. Recent theoretical calculations have reported that N vacancies are the most likely to form, and that this state forms over the E_V with +3 charge state. It seems to correspond to the tail state detected from 3.0 eV to 2.4 eV in the PDS spectra with In composition of 5% and 8% in Fig. 3.

The binding energy of In 4d is lower than that of Ga 3d.[31] The valence band spectra of $In_xGa_{1-x}N$ films observed by HAX-PES were shifted to lower binding energy with an increase of In composition, due to In 4s orbital hybridized with N 2p. The band offset between InN and GaN was about 1.5 eV.[32] As the In composition increases, the Urbach-like energy increases due to the larger fluctuation of In atom arrangement. The change of slope near the valence band in the PDS spectra in Figs. 3(b) and 3(c) might be formed by both the tail state caused by V_N and the shift of the hybridized In 4s orbital. No change was observed in the PDS spectrum of Fig. 3(d) for $In_{0.12}Ga_{0.88}N$ film. This is because the V_N states may be covered by larger Urbach-like energy. (Further increase of In composition InGaN film with more than 50% of In caused In ad-layer on the surface which was detected below the conduction band.[32]) Photoluminescence might occur around V_N with +3-charge where the

In composition may be locally high. Consequently, the difference between the absorption edge and the PL peak energy increases as the In composition increases.

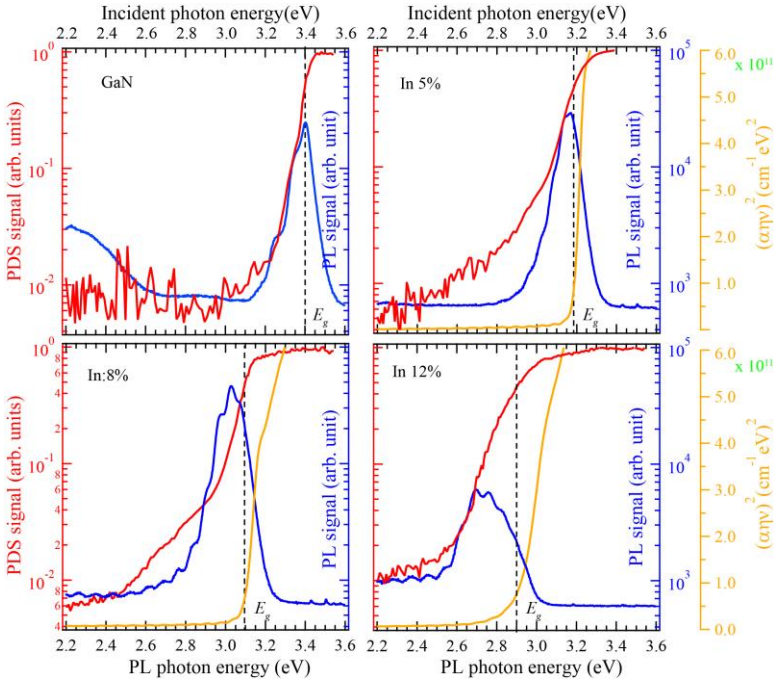

Fig. 3 PDS (red), PL (blue) and Tauc plot (green) for (a) GaN, (b) $In_{0.05}Ga_{0.95}N$, (c) $In_{0.08}Ga_{0.92}N$ and (d) $In_{0.12}Ga_{0.88}N$ film grown on GaN/sapphire substrates.

3.6 PL-PDS correlation for GaN film thickness

Yellow luminescence (YL) was observed in PL from GaN (Fig. 3(a)), while no YL from InGaN films with larger Urbach-like energy was detected. It was thought that a sample which emitted no light such as YL related to the defect levels in the band gap (in-gap emission) would be good. Interestingly, no in-gap emission was observed from InGaN, which has a higher defect density than GaN. The in-gap emission from ion-implanted sample induced by thermal annealing has been used as an indicator of structural recovery.[33] Therefore, it seems that absence of in-gap emission is not necessarily an indicator of the degree of defect density in the sample. Since PDS and PL are two sides of the same coin in terms of radiative and non-radiative recombination, we consider the emission intensity in the band gap of GaN and the PDS signal intensity in this section.

Figures 4(a) and (b) show PL and PDS spectra of GaN thin films grown on AlN templates /sapphire substrates, and Figs. 4(c) and (d) show those of GaN grown on low-temperature GaN buffer layers on sapphire substrates. PL and PDS measurements of GaN films grown on each substrate for different times were performed. The intensities of the PL at the band edge were almost same. The in-gap emission intensity is clearly stronger for the GaN films on AlN templates, and the PDS intensity in the band gap is lower. Since the PDS intensity in the band gap decreases as the film thickness increases, the PL intensity of YL and GL emission increases. The peak intensity in the gap of the PDS spectrum and the energy position of the emission peak are almost the same. It can be interpreted that emission from inside the gap is observed because the non-radiative recombination of the level inside the gap is reduced.

The Urbach-like energy of PDS spectra of GaN sample on LT-GaN buffer layer was not improved with an increase of growth time. The PDS signal intensity in the band gap of GaN film grown for ~300 sec was almost same as that on the AlN template, but the in-gap emission intensity was lower. For the PDS spectrum of GaN grown for 1 hour on LT-GaN buffer layer, the Urbach-like energy was improved and the PDS signal intensity at 2.8 eV decreased. The in-gap emission of blue luminescence (BL) was observed in the PL spectrum. When the crystalline quality of the ion-implanted sample was improved by thermal annealing (Urbach-like energy decreased), the in-gap emissions were observed.[34)] Therefore, it seemed that the Urbach-like energy was related to the in-gap emission. Considering that the in-gap emission was caused by the band edge luminescence from the PLE measurement,[34)] it was thought that the Urbach-like energy would be involved for the electrons excited at the band edge to diffuse to the radiative levels in the band gap. In the current situation where the defect level in the band gap cannot be completely eliminated, it seems necessary to consider the correlation between the Urbach-like energy and the in-gap emission.

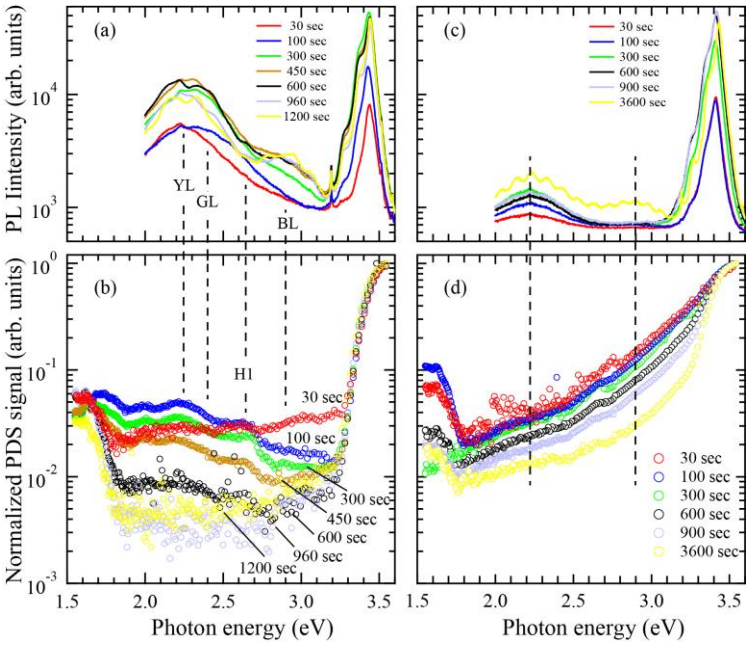

Fig. 4 (a) PL and (b) PDS spectra for GaN films grown for various time on AlN templates on sapphire. (c) PL and (d) PDS spectra for GaN films grown on sapphire substrate using LT-GaN buffer layer.

4. Conclusions

This paper describes the challenges and advantages in evaluating III-V nitride semiconductors by PDS. The method of PDS has the feature that it can detect the defect energy level in the bandgap over a wide range from 1.0 eV to 4.9 eV without forming electrodes. The PDS method was available for electrically and optically inactive materials such as ion-implanted GaN and AlGaN with high insulative property. Considering the radial distribution determined by XAFS, we believe that the Urbach-like energy and tail state near the band edge of the PDS spectrum of the InGaN film may indicate the non-uniformity of In atomic arrangement and the V_N, respectively. From PDS (non-radiative) and PL (radiative) measurements for GaN films, it was suggested that the Urbach-like energy might be related to the emission from the defect levels. It is expected that PDS characterization would be one of the useful tools for discussing defects in III-V nitrides.

Acknowledgments

XAFS measurements were performed at BL01B1 in SPring-8 (proposal no. 2017B1428). Author thanks Dr. K. Saito, Sping-8 for supporting the XAFS experiment, and prof. T. Honda, Kogakuin-University for valuable discussions.

References

1) S. Nakamura, T. Mukai, and M. Senoh, Appl. Phys. Lett. **64**, 1687 (1994).

2) H. Hirayama J. Appl. Phys. **97**, 091101 (2005).

3) H. Amano et al., Phys. D: Appl. Phys. **53** 503001 (2020).

4) D. Iida, Z. Zhuang, P. Kirilenko, M. Velazquez-Rizo, M. A. Najmi, K. Ohkawa, Appl. Phys. Lett. **116**,162101 (2020).

5) M. A. Khan, A. Bhattarai, J. N. Kuznia, D. T. Olson, Appl. Phys. Lett. **63**, 1214 (1993).

6) T. Oka, T. Ina, Y. Ueno, and J. Nishii, Appl. Phys. Express **8**, 054101 (2015).

7) K. Hiramatsu, S. Itoh, H. Amano, I. Akasaki, N. Kuwano, T. Shiraishi, K. Oki, J. Cryst. Growth **115**, 628 (1991).

8) M. Sumiya, K. Yoshimura, K. Ohtuska and S. Fuke, Appl. Phys. Lett. **76**, 2098 (2000).

9) A. Uedono, S. F. Chichibu, Z. Q. Chen, M. Sumiya, R. Suzuki, T. Ohdaira, T. Mikado, T. Mukai, S. Nakamura, J. Appl. Phys. **90** 181 (2001).

10) P. Šcˇajev, K. Jarašiūnas, S. Okur, Ü. Özgür, H. Morkoç, J. Appl. Phys. **111**, 023702 (2012).

11) P. Hacke; T. Detchprohm; K. Hiramatsu; N. Sawaki; K. Tadatomo; K. Miyake, J. Appl. Phys. **76** 304 (1994).

12) Boccara A. C., Fournier D., Jackson W. B. and Amer N. M. Opt. Lett. **5** 377 (1980)

13) M. Sumiya, S. Ueda, K. Fukuda, Y. Asai, Y. Cho, L. Sang, A. Uedono, T. Sekiguchi, T. Onuma and T. Honda, Appl, Phys. Express **11**, 021002 (2018)

14) Nakano Y., Lozac'h M., Matsuki N., Sakoda K. and Sumiya M. 2011 J. Vac. Sci. Technol. B **29** 023001 (2011).

15) A. Armstrong, A. Chakraborty, J. S. Speck, S. P. DenBaars, U. K. Mishra, S. A. Ringel, Appl. Phys. Lett. **89**, 262116 (2006).

16) Tran Thien Duc, Galia Pozina, Erik Janzen, and Carl Hemmingsson, J. Appl. Phys. **114**, 153702 (2013).

17) M. Sumiya, H. Fujikura, Y. Nakano, S. Yashiro, Y. Koide, and T. Honda, submitted to Appl. Phys. Lett.

18) M.Buffolo, A. Caria, F. Piva, N. Roccato, C. Casu, C. De Santi, N. Trivellin, G. Meneghesso, E. Zanoni, and M. Meneghini, Phys. Status Solidi A, 2100727 (2022).

19) B. Brunwin, B. Hamilton, P. Jordan, and A. Peker, Electon. Lett.. **15**, 349 (1979).

20) T. Nakano, K. Kawakami, A. A. Yamaguchi. Proc. of SPIE - The International Society for Optical Engineering 9748, 97481W (2016).

21) T. Hata, T. Hatsuda and T. Komatsu, Jpn. J. Appl. Phys. **24** 1463 (1985).

22) A. Skumamch, A. Frova and N. M. Amer, Solid State Commu. **54**, 597 (1985).

23) E. Bustarret, D. Jousse, C. Chaussat, F. Boulitrop, J.Non-Crys. Solids **77 & 78**, 295 (1985).

24) S. Nonomura, S. Hattori, H. Hayashi, T. Itoh, S. Nitta, J. Non-Crys. Solids **114**, 729 (1989).

25) A. Asano and M. Stutzmann, J. Appl. Phys. **70** 5025 (1991).

26) M. Sumiya, K. Fukuda, S. Takashima, S. Ueda, T. Onuma, T. Yamaguchi, T. Honda, A. Uedono, J. Crys. Growth, **511**, 15 (2019).

27) N. Pant, A. Kulkarni, M. Yanagida, Y. Shirai, S. Yashiro, M. Sumiya, T. Miyasaka, K. Miyano, ACS Appl. En. Mat. **4**, 4530 (2021).

28) T. Mikie, M. Hayakawa, K. Okamoto, K. Iguchi, S. Yashiro, T. Koganezawa, M. Sumiya, H. Ishii, S. Yamaguchi, A. Fukazawa, and I. Osaka, Chem. Mater. **33**, 8183 (2021).

29) T. Mikie, K. Okamoto, Y. Iwasaki, T. Koganezawa, M. Sumiya, T. Okamoto, and I. Osaka, Chem. of Mat. **34**, 2717 (2022).

30) W. R. L. Lambrecht, B. Segall, S. Strite, G. Martin, A. Agarwal, H. Morkoc, and A. Rockett, Phys. Rev. B 50, 14155 (1994).

31) M. Lozac'h, S. Ueda, S. Liu, H. Yoshikawa, L. Sang X. Wang, B. Shen, K. Sakoda, K. Kobayashi and M. Sumiya, Sci. Tech. Adv. Mat. **14**, 015007 (2013).

32) M. Sumiya, S. Ueda, Y. Harada, T. Yamaguchi, X. Wang, and Liwen Sang (unpublished data).

33) K. Kojima, S. Takashima, M. Edo, K Ueno, M. Shimizu, T. Takahashi, S. Ishibashi, A. Uedono, and S. F. Chichibu, Appl. Phys. Express **10**, 061002 (2017)

34) M. Sumiya, K. Fukuda, H. Iwai, T. Yamaguchi, T. Onuma, T. Honda, AIP Advances **8**, 115225 (2018).